E. coli JM83 damages the mucosal barrier in Ednrb knockout mice to promote the development of Hirschsprung-associated enterocolitis via activation of TLR4/p-p38/NF-κB signaling

ZEBING ZHENG[1], MINGJUAN GAO[2], CHENGYAN TANG[2], LU HUANG[2], YUAN GONG[2], YUANMEI LIU[2] and JIAN WANG[1]

[1]Department of Pediatric Surgery, Children's Hospital of Soochow University, Pediatric Research Institute of Soochow University, Suzhou, Jiangsu 215123; [2]Department of Pediatric Surgery, Affiliated Hospital of Zunyi Medical University, Zunyi, Guizhou 563000, P.R. China

Received December 9, 2021; Accepted February 24, 2022

DOI: 10.3892/mmr.2022.12684

Abstract. Hirschsprung-associated enterocolitis (HAEC) is characterized by intestinal mucosal damage and an imbalance in the intestinal microbiota. Recent studies have indicated that the TLR4/p-p38/NF-κB signaling pathway in the intestine is of great importance to intestinal mucosal integrity. The present study aimed to investigate the role of TLR4/phosphorylated (p-)38/NF-κB signaling in the pathogenesis of HAEC in *E. coli* JM83-infected endothelin receptor B (Ednrb)$^{-/-}$ mice. Ednrb$^{-/-}$ mice were infected with *E. coli* JM83 by oral gavage to establish the HAEC model. Wild-type and Ednrb$^{-/-}$ mice were randomly divided into uninfected and *E. coli* groups. The role of TLR4/p-p38/NF-κB signaling was further evaluated by *in vivo* and *in vitro* analyses. The activation of the TLR4/p-p38/NF-κB signaling pathway induced by *E. coli* JM83 resulted in HAEC in Ednrb$^{-/-}$ mice, which was evidenced by a significant increase in the expression of TNF-α, TGF-β and IL-10, and a decreased density of F-actin protein expression. TLR4 knockdown reduced the severity of enterocolitis and attenuated the expression of IL-10, TNF-α and TGF-β, whilst increasing the density of F-actin protein in Ednrb$^{-/-}$ mice after *E. coli* infection. These results indicated that *E. coli* JM83 activates TLR4/p-p38/NF-κB signaling in Ednrb$^{-/-}$ to promote the development of HAEC. Thus, inhibition of this signaling pathway may benefit the treatment and prevention of HAEC.

Correspondence to: Professor Jian Wang, Department of Pediatric Surgery, Children's Hospital of Soochow University, Pediatric Research Institute of Soochow University, 92 Zhongnan Street, Suzhou Industrial Park, Jingde Road, Suzhou, Jiangsu 215123, P.R. China
E-mail: wj196312@vip.163.com

Abbreviations: HAEC, Hirschsprung-associated enterocolitis; HSCR, Hirschsprung disease; TLR4, Toll-like receptor 4; WT, wild-type; Ednrb, endothelin receptor B

Key words: Hirschsprung-associated enterocolitis, TLR4, mucosal barrier, endothelin receptor B

Introduction

Hirschsprung-associated enterocolitis (HAEC) is the most common complication of Hirschsprung disease (HSCR) (1,2), which may occur during the preoperative or postoperative stages of surgery, even after definitive pull-through surgery (3). Accumulating clinical evidence suggests that abnormalities in the intestinal microbiome, impaired intestinal mucosal barrier function, altered systemic immune system function and bacterial translocation are all possible causes of HAEC (4-6). The intestinal tract is the most active immune organ in the human body and it is constantly challenged by a large number of antigens. A previous study indicated *Clostridium difficile*, *E. coli* and certain viruses may be causative agents of enterocolitis development (7). However, the mechanisms by which gut microbes influence the mucosal barrier and the development of pathogenic bacteria-mediated HAEC remain to be fully elucidated; an increasing number of studies have investigated the possible implication of *Clostridium difficile* as a pathogen of HAEC but remain inconclusive (8,9). According to the results of Illumina-MiSeq high-throughput sequencing for characterization of intestinal microbiomes of HAEC (10), *E. coli* was the most prominent genus detected in patients with HAEC and recurrence of HAEC (11). However, the role of *Clostridium* species as a cause of HAEC remains controversial. Therefore, *E. coli* was selected as the preferred pathogen in the present study (9-11).

Toll-like receptor 4 (TLR4) is a transmembrane protein, which has important effects in initiating inflammatory reactions (12). A recent study suggested that defective murine TLR4 was responsible for lipopolysaccharide (LPS) hyporesponsiveness in two mouse strains, and furthermore, a study in TLR4-deficient mice revealed that TLR4 was essential for LPS-induced inflammatory signaling (13). A previous study reported that the dysregulated expression of TLR4 signaling transduction led to uncontrolled colitis, which was associated with the loss of mucosal integrity, development of ulcerations

and colonic bleeding (14), consistent with what is observed in patients with HAEC. Emerging evidence has indicated that TLR4 expression is upregulated in several intestinal inflammatory diseases, including inflammatory bowel colitis (15) and necrotizing enterocolitis (16). When TLR4 is engaged by its ligands, the downstream signaling pathways, including the NF-κB and MAPK p38 [phosphorylated (p-)p38] pathways, are activated; this activation is essential for the initiation of an inflammatory response by promoting and/or modulating the transcription and translation of inflammation-related genes, such as IL-6, TNF-α and IL-1β (17). Inhibition of NF-κB has also been indicated to protect against colonic epithelium damage and/or promote epithelial repair (18,19).

In the present study, it was hypothesized that the pathogenic organism *E. coli* JM83 promotes HAEC development through TLR4/p-p38/NF-κB signaling, influencing intestinal mucosal barrier integrity. Thus, whether TLR4/p-p38/NF-κB signaling participates in the pathogenesis of HAEC during the invasive infection of endothelin receptor B (Ednrb)$^{-/-}$ mice with *E. coli* JM83 (used as a model of HAEC) was assessed in the present study.

Materials and methods

Animals. Female wild-type (WT; age, 8 weeks; weight, 16-19 g; n=20), female Ednrb$^{flex3/flex3}$ (age, 8 weeks; weight, 15-19 g; n=8) mice and male Ednrb$^{flex3/+}$ (age, 8 weeks; weight, 15-19 g; n=8). Endothelin receptor B-null mice (Ednrb$^{flex3/flex3}$ and Ednrb$^{flex3/+}$) were established using C57/B6J mice. All mice were purchased from the Institute of Model Animals of Wuhan University (Wuhan, China). In brief, after mating Ednrb$^{flex3/+}$ mice with Ednrb$^{flex3/flex3}$ mice, the homozygotes (herein referred to as Ednrb$^{-/-}$) were easily distinguished from the WT and heterozygote littermates (herein referred to as Ednrb$^{+/+}$ and Ednrb$^{+/-}$, respectively) by the white fur color and gradually enlarging abdomens (due to the absence of ganglion cells at the end of the rectum). Ednrb$^{+/+}$ and Ednrb$^{+/-}$ mice had a normal phenotype and did not develop aganglionosis. Therefore, 20 Ednrb$^{+/+}$ or Ednrb$^{+/-}$ animals were randomly assigned to the WT group. A total of 20 Ednrb$^{-/-}$ animals were obtained for the present study that displayed distal colonic aganglionosis involving 5-10 mm of the colon. Naive mice were defined as WT and Ednrb$^{-/-}$ mice without any intervention. All experiments involving animals were performed in a specific pathogen-free environment and were approved by the Institutional Animal Research Committee of Zunyi Medical University (Zunyi, China; approval no. IACUC-20191025028) and were in accordance with the Zunyi Medical University Guidelines for Animal Care. Animals were maintained under a 12-h light/dark cycle at a temperature of 22±2˚C in an air-conditioned room, and were given access to food and water *ad libitum*. Male and female mice were raised separately. A total of eight mice survived more than 5 weeks; however, two mice died of abdominal distension, diarrhea, and severe dehydration before the date of sacrifice in the Ednrb$^{-/-}$ group infected with *E. coli*. All mice were sacrificed 5 weeks after modeling. Isoflurane inhalation anesthesia was used (induction concentration, 3%; maintenance concentration, 1%), followed by collection of the colon and blood. Subsequently, mice were sacrificed by CO_2 asphyxia (50% CO_2 volume displacement rate). When cessation of the heartbeat and breathing of the mice was verified, and no reflexes were detected, the death of mice was confirmed.

Bacterial strains. The *E. coli* JM83 (Jackson Laboratory) strain was cultured on trypsin soybean agar plates (BD Biosciences) supplemented with 5% sheep blood (BD Biosciences), which was in turn supplemented with 0.2% yeast extract (Merck KGaA) at 37˚C with 5% CO_2 (durations indicated in individual experiments).

Establishment of the HAEC model. WT and Ednrb$^{-/-}$ mice were infected with 0.1 ml Lb broth containing 1x10^9 colony-forming units of *E. coli* JM83 (Jackson Laboratory) by oral gavage to establish the WT+*E. coli* (n=5) and Ednrb$^{-/-}$+*E. coli* (n=5) groups. The colon samples from Ednrb$^{-/-}$+*E. coli* mice were stored at -80˚C and embedded in paraffin for subsequent H&E as well as immunofluorescence staining analysis (described below) to verify the establishment of the HAEC model. Inflammatory cell infiltration of the crypts (cryptitis and crypt abscesses) was lighter in HAEC mice than in human patients with HAEC. The WT and Ednrb$^{-/-}$ mice were used as the control groups. The severity of HAEC was evaluated according to the modified grading system reported by Porokuokka *et al* (20) to reflect the epithelial pathology in HAEC mice. Parts of the small bowel (jejunum and ileum) or large bowel (cecum and colon) were excised by separation from the mesentery to prepare a single intestinal cell suspension.

si-RNA transfection. In order to knockdown TLR4 expression in WT+*E. coli* and Ednrb$^{-/-}$+*E. coli* mice, small interfering RNA (siRNA) targeting TLR4 (si-TLR4) and the corresponding negative control (siRNA-NC) were used to generate WT+siRNA-NC+*E. coli* (n=5), WT+si-TLR4+*E. coli* (n=5) and Ednrb$^{-/-}$+si-TLR4+*E. coli* (n=5) mouse groups (21). In brief, after anesthetization with isoflurane (induction concentration, 3%; maintenance concentration, 1%), 20 nmol/kg siRNA was injected into the caudal vein twice a week to target TLR4. The sequences of the siRNAs were as follows: si-TLR4 sense, 5'-UUCGAGACUGGACAAGCC-3' and antisense, 5'-UGGCUUGUCCAGUCACGA-3'; siRNA-C sense, 5'-UUC UCCGAACGUGUCACGUTT-3' and antisense, 5'-TTAAGA GGCUUGCACAGUGCA-3' (100 nM; Guangzhou RiboBio Co., Ltd.). Ednrb$^{-/-}$+*E. coli* mice were used as a control group. Knockdown of the TLR4 gene was confirmed at the protein level by western blot analysis.

H&E staining and immunohistochemistry (IHC). The colon sections were removed following euthanasia and cut into 3-mm sections, stained with H&E at room temperature and imaged using light microscopy (Nikon Corporation; magnification, x200). The stained sections were assigned an inflammatory score in a blinded manner, as previously described (20). TLR4 protein expression levels were detected by IHC. The IHC sections were incubated overnight at 4˚C in primary antibody solution containing anti-human TLR4 antibody (cat. no. A0456; final dilution, 2 μg/l; 1:200; OriGene Technologies, Inc.), and a biotin-streptavidin HRP detection system for 12 h. The sections were incubated with biotinylated goat anti-rabbit IgG (cat. no. 2019629; 1:200 dilution; OriGene Technologies, Inc.)

at room temperature for 30 min, and followed by probing with an HRP-conjugated anti-rabbit IgG secondary antibody (cat. no. 40295G; 1:200; BIOSS) at room temperature for 30 min. Negative controls were treated with PBS instead of primary antibodies. All sections were observed using a light microscope (Olympus BH-2; Olympus Corporation; magnification, x100).

Immunofluorescence. For immunofluorescence staining, colon tissues were separated from mice. Colon tissues were fixed in PBS/4% paraformaldehyde and 10% sucrose solution at 4˚C for 1 h, followed by cryoprotection in PBS/30% sucrose (Merck KGaA) for 3 days at 4˚C. Tissue sections were cut into 20-mm sections using a Leica Cryostat Microtome, blocked using a Streptavidin/Biotin Blocking kit (Vector Laboratories, Inc.) according to the manufacturer's protocol and stored at -80˚C until required. Colon tissue samples were stained with either mouse or rabbit anti-F-actin antibodies (cat. no. 8927; 1:2,000 dilution; Merck KGaA) for 3 h at room temperature and counterstained with DAPI (cat no. 6982; BioLegend, Inc.) for 5 min at room temperature. Sections were observed using a FV1000 laser-scanning confocal microscope (Olympus Corporation; magnification, x200).

Western blot analysis. Western blot analysis was performed following protein extraction using RIPA lysis buffer (Beijing Solarbio Science & Technology Co., Ltd.) according to the manufacturer's protocol, and protein concentrations were measured using an Enhanced Bicinchoninic Acid Protein Assay kit (Beyotime Institute of Biotechnology). Tissue protein extracts (120 μl) were mixed with SDS buffer (Beyotime Institute of Biotechnology) and heated at 90˚C for 5 min. Proteins (30 μg per lane) were resolved using 12% SDS-PAGE and were subsequently transferred to PVDF membranes (MilliporeSigma). The membranes were blocked with 5% fat-free milk in Tris-buffered saline (TBS) for 45 min at room temperature and washed with TBS containing Tween-20 (TBST), and then incubated with the following primary rabbit anti-mouse antibodies: Anti-TLR4 (cat. no. ab22048), anti-NF-κBp65 (cat. no. ab16502), anti-p-p38 (cat. no. ab31828), anti-p38 (cat. no. ab2749) (all from Abcam; 1:200 dilution) and anti-GAPDH (cat. no. ab60004; Abcam; 1:200 dilution) at 4˚C for 16 h. The membranes were washed with TBST three times and subsequently incubated with secondary antibodies [anti-rabbit IgG (cat. no. sc-2357; 1:1,000 dilution) or anti-mouse IgG (cat. no. sc-2942; 1:1,000 dilution), both from Beyotime Institute of Biotechnology] for 2 h at room temperature. The protein bands were visualized using an ECL Plus kit (cat. no. E1116; Beyotime Institute of Biotechnology) and the Fusion FX7 Spectra multifunction imaging system (Vilber Lourmat) was used to detect bands. ImageJ version 1.8.0 (National Institutes of Health) was used for densitometric analysis.

Reverse transcription-quantitative PCR (RT-qPCR). For RT-qPCR, total RNA was extracted from colon tissues and macrophages using TRIzol® reagent (Invitrogen; Thermo Fisher Scientific, Inc.) according to the manufacturer's protocol. A NanoDrop 2000 spectrophotometer (Thermo Fisher Scientific, Inc.) was used for RNA concentration analysis. qPCR amplification was subsequently performed on an ABI 7900HT Real-Time PCR Detection system (Applied Biosystems; Thermo Fisher Scientific, Inc.) to measure the mRNA expression levels. The thermocycling conditions were as follows: Initial denaturation at 50˚C for 2 min and 95˚C for 10 min; followed by 40 cycles of 95˚C for 15 sec and 60˚C for 60 sec. Expression levels were calculated using the $2^{-\Delta\Delta Cq}$ method (22). Relative expression levels were normalized to GAPDH. The primer sequences for each gene were as follows: TLR4 forward, 5'-CATGGATCA GAAACTCAGCAAAGTC-3' and reverse, 5'-CATGCCATGCCTTGTCTTCA-3'; p38 forward, 5'-CGACTTGCTGGAGAAGATGC-3' and reverse, 5'-TCC ATCTCTTCTTGGTCAAGG-3'; NF-κB forward, 5'-AGA CCTGGAGCAAGCCATTAG-3' and reverse, 5'-CGGACC GCATTCAAGTCATAG-3'; and GAPDH forward, 5'-GAC GGCCGCATCTTCTTGT-3' and reverse, 5'-CACACCGAC CTTCACCATTTT-3'.

ELISA. The levels of IL-10, TNF-α and TGF-β in colon tissues were measured using commercially available ELISA kits [IL-10 (cat. no. H009), TNF-α (cat. no. H052) and TGF-β (cat. no. H034); all from Nanjing Jiancheng Bioengineering Institute] according to the manufacturer's instructions.

Muscularis macrophage (MM) culture, treatment and transfection. The colons of WT and Ednrb$^{-/-}$ mice were carefully excised and separated from the mesentery, cleaned and washed with Hank's Balanced Salt Solution (HBSS) $Mg^{2+}Ca^{2+}$ (Gibco; Thermo Fisher Scientific, Inc.). The colon tissues were opened in two, cut into 2-mm pieces and digested with 400 U/ml collagenase D (Gibco; Thermo Fisher Scientific, Inc.) supplemented with HBSS $Mg^{2+}Ca^{2+}$, 2% FBS (Gibco; Thermo Fisher Scientific, Inc.) 1X NaPyr + 25 mM HEPES + 50 μg/ml DNase I + 2.5 U/ml dispase (Shanghai Maokang Biotechnology Co., Ltd.) at 4˚C for 20 min. The digested tissue was homogenized and washed. Subsequently, the dissociated tissue was filtered through a 70-μm mesh cell strainer, washed with HBSS $Mg^{2+}Ca^{2+}$ and incubated with PBS containing 1% BSA, 10 mM EDTA, 0.02% sodium azide containing Fc block and antibodies against CD16/CD32 (cat. no. A0847; 1:200 dilution) (all from Gibco; Thermo Fisher Scientific, Inc.) at 4˚C for 30 min (23), washed and stained with fluorophore-conjugated antibodies in PBS/2% FBS for 30 min at 4˚C. The obtained MMs were maintained in DMEM (Gibco; Thermo Fisher Scientific, Inc.). siRNAs targeting TLR4 for knockdown TLR4 expression in Ednrb$^{-/-}$ MMs, and corresponding siRNA-NC for WT MMs, synthesized by Guangzhou RiboBio Co., Ltd. were transfected into the cells. The cell groups included: WT+ siRNA-NC group, WT group, Ednrb$^{-/-}$ group and Ednrb$^{-/-}$ + si-TLR4 group. A total of 2 μg/ml siRNA was transfected into MMs at 37˚C for 10 h using Lipofectamine® 2000 transfection reagent (Invitrogen; Thermo Fisher Scientific, Inc.) according to the manufacturer's protocol. At 48 h post-transfection, the WT+siRNA-NC MMs were supplemented with 10% PBS, while the WT, Ednrb$^{-/-}$ and Ednrb$^{-/-}$+si-TLR4 MMs were supplemented with 100 ng/ml *E. coli* JM83. All cells (2,000 cells per well) were seeded in 96-well culture plates. WT+*E. coli* and Ednrb$^{-/-}$+*E. coli* were control groups. Cell Counting Kit-8 reagent was used according to the manufacturer's instructions (Beyotime Institute of Biotechnology) after 0, 24 or 48 h to assess cell proliferation. The expression of TLR4/p-p38/NF-κB signaling

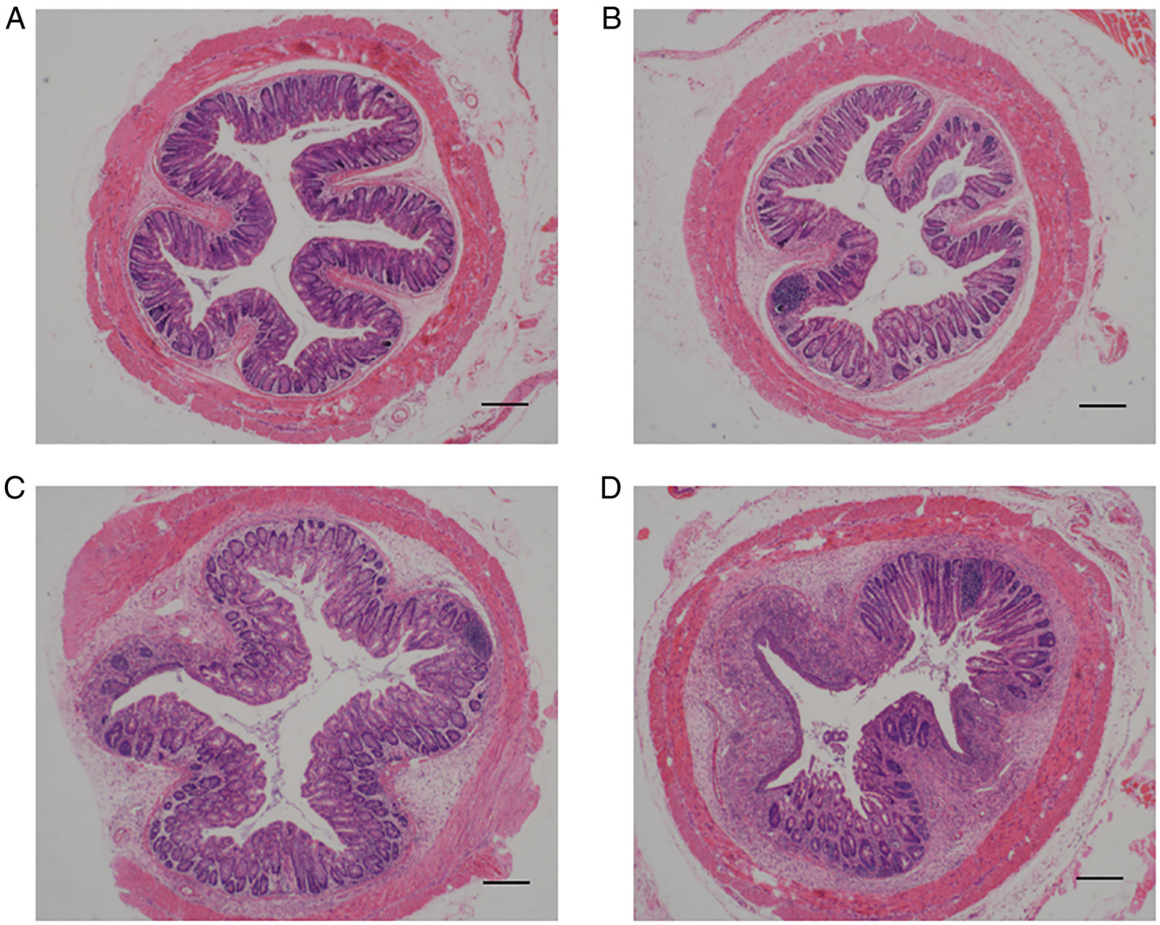

Figure 1. *E. coli* and Ednrb deficiency promote the development of Hirschsprung-associated enterocolitis. The colon tissues were collected at 5 weeks after modeling. (A) WT group; (B) *E. coli*-infected WT group; (C) Ednrb$^{-/-}$ group; and (D) *E. coli*-infected Ednrb$^{-/-}$ group (5 mice per group). Hematoxylin and eosin staining was performed to assess histopathological changes (scale bar, 100 μm). Ednrb, endothelin receptor B; WT, wild-type.

pathway members was assessed by western blot analysis and RT-qPCR, and the collected media were analyzed for IL-10, TNF-α and TGF-β protein levels by ELISA.

Statistical analysis. SPSS version 19.0 (IBM Corp.) and GraphPad Prism version 8.0 (GraphPad software Inc.) were used for statistical analysis. Normally distributed data are presented as the mean ± standard deviation and were statistically analyzed using one-way ANOVA, followed by Tukey's post hoc test. P<0.05 was considered to indicate a statistically significant difference.

Results

The TLR4/p-p38/NF-κB signaling pathway participates in the pathogenesis of HAEC in Ednrb$^{-/-}$ mice. The Ednrb-null mouse (Fig. S1A and B) was used to resemble the pathological features of HSCR, including aganglionosis in the rectum and distal colon, as well as enterocolitis (21). First, WT and Ednrb$^{-/-}$ mice were infected with *E. coli* JM83 and inflammation scores in the colon were histologically assessed. As presented in Fig. 1, naive Ednrb$^{-/-}$ mice developed enterocolitis spontaneously after 5 weeks (Fig. 1C), whereas Ednrb$^{-/-}$ mice infected with *E. coli* devloped enterocolitis after 3 weeks. The degree of epithelial damage and leukocyte infiltration in *E. coli*-infected Ednrb$^{-/-}$ mice were more than naive Ednrb$^{-/-}$ mice when they were sacrificed at 5 weeks (Fig. 1D). By contrast, WT mice infected with *E. coli* (Fig. 1B) only developed mild inflammation in the colon compared with WT mice (Fig. 1A).

Ednrb increases TLR4/p-p38/NF-κB signaling to promote enterocolitis. As presented in Fig. 2, IHC analysis revealed intense brown staining, resembling TLR4 expression in the colon of Ednrb$^{-/-}$ (Fig. 2C) and *E. coli*-infected Ednrb$^{-/-}$ mice (Fig. 2D), compared with WT (Fig. 2A) and *E. coli*-infected WT mice (Fig. 2B). The average optical density values of TLR4 in *E. coli*-infected Ednrb$^{-/-}$ mice were higher than those in the Ednrb$^{-/-}$ and WT mice (Fig. 2E). Western blot analysis and RT-qPCR further confirmed that the protein and mRNA levels of TLR4, NF-κB and p-p38 were significantly increased in Ednrb$^{-/-}$ and *E. coli*-infected Ednrb$^{-/-}$ mice (P<0.05 vs. WT and *E. coli*-infected WT mice), with no significant difference identified between the Ednrb$^{-/-}$ and *E. coli*-infected Ednrb$^{-/-}$ mice (P>0.05; Fig. 3A-C). In addition, the expression levels of TNF-α, TGF-β and IL-10 were increased in Ednrb$^{-/-}$ and *E. coli*-infected Ednrb$^{-/-}$ mice, compared with those in WT and *E. coli*-infected WT mice (P<0.05; Fig. 3D). Of note, *E. coli*-infected Ednrb$^{-/-}$ mice exhibited markedly higher TNF-α, TGF-β and IL-10 levels than Ednrb$^{-/-}$ mice (P<0.05; Fig. 3D).

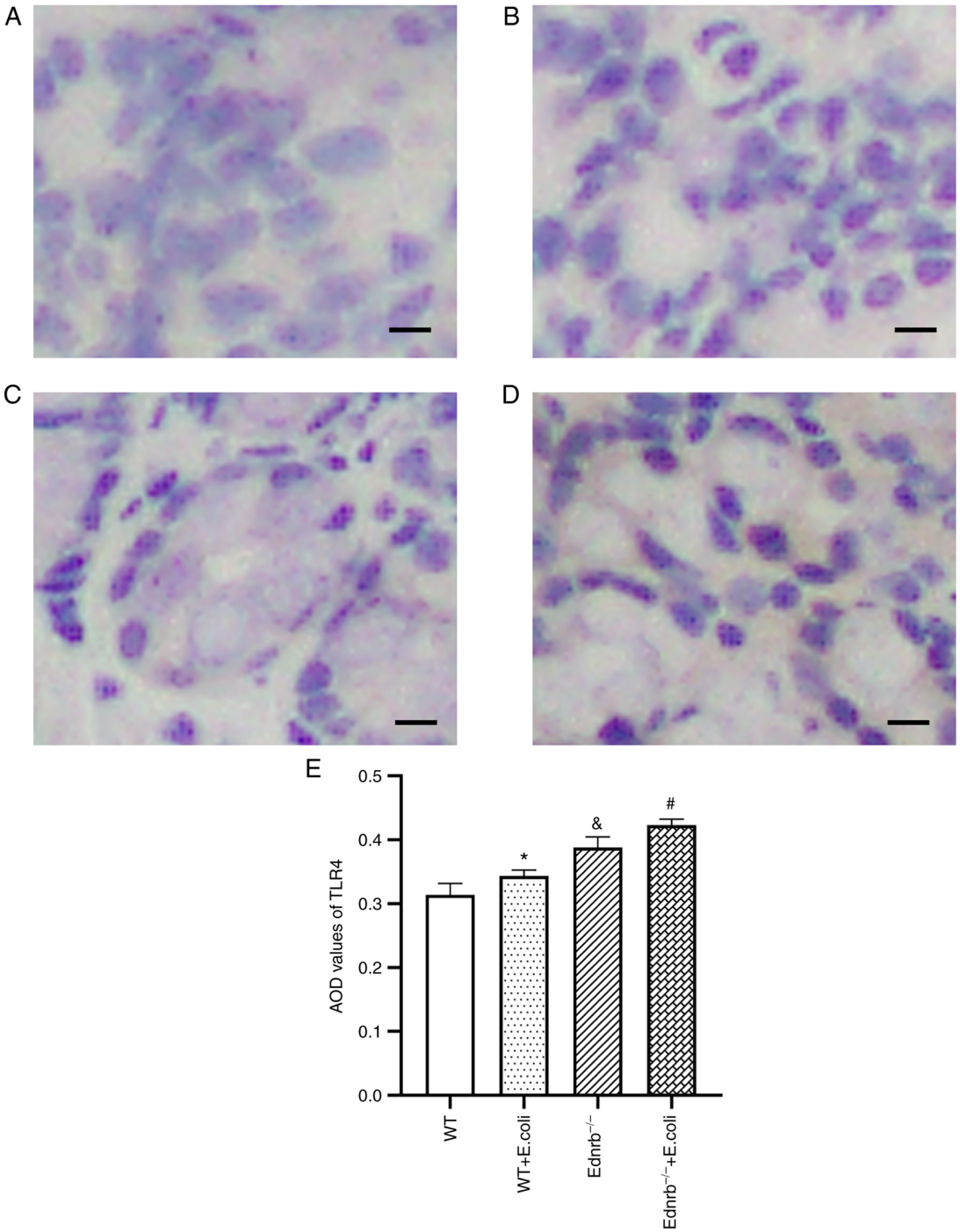

Figure 2. Representative immunohistochemical staining for TLR4. (A) WT group; (B) *E. coli*-infected WT group; (C) Ednrb$^{-/-}$ group; and (D) *E. coli*-infected Ednrb$^{-/-}$ group (5 mice per group; scale bar, 200 μm). (E) Quantification of the immunohistochemical staining for TLR4. *P<0.05 vs. WT group; $^{\&}$P<0.05 vs. *E. coli*-infected WT group; $^{\#}$P<0.05 vs. Ednrb$^{-/-}$ group. Ednrb, endothelin receptor B; WT, wild-type; TLR4, toll-like receptor 4; AOD, average optical density.

TLR4 knockdown reverses intestinal inflammation. To assess the extent of damage to the intestinal mucosal barrier and the role of TLR4/p-p38/NF-κB signaling in *E. coli* JM83 infection-induced HAEC, the severity of enterocolitis and cytoskeletal F-actin expression was assessed following TLR4 knockdown in WT and Ednrb$^{-/-}$ mice. It has been reported that changes in F-actin in the intestinal epithelial cytoskeleton may occur as a mechanism of damage to intestinal barrier function (24). As indicated in Fig. 4, a marked interruption in mucosal structures was present, and large numbers of inflammatory cells and abscesses were observed to have infiltrated the mucosa and sub-mucosa upon *E. coli* infection in Ednrb$^{-/-}$ mice (Fig. 4C), whereas the severity of *E. coli* infection-induced enterocolitis was markedly alleviated in Ednrb$^{-/-}$ mice following TLR4 knockdown (Fig. 4D). In addition, the mild degree of inflammation in the colon observed in *E. coli*-infected WT+siRNA-NC mice (Fig. 4A) was almost completely reversed by TLR4 knockdown (Fig. 4A). F-actin expression was increased in the cytoplasm of intestinal epithelial cells, alongside increased tight junction integrity

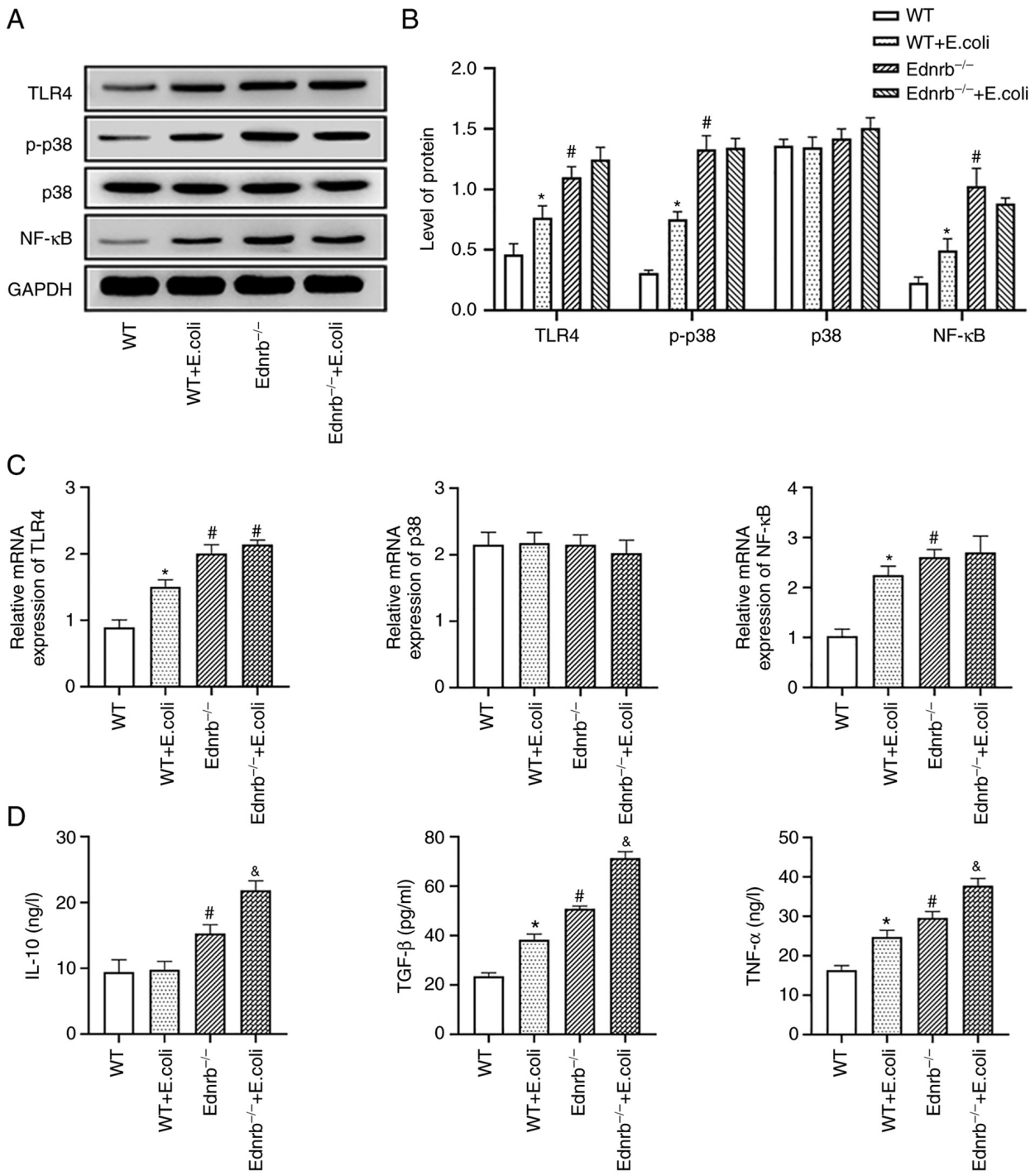

Figure 3. TLR4/p-p38/NF-κB signaling is involved in the pathogenesis of Hirschsprung-associated enterocolitis following Ednrb knockout. (A and B) Western blot analysis of TLR4, p-p38, p38 and NF-κB protein expression in colonic tissues. (A) Representative western blot image and (B) quantified expression levels (n=5 per group). (C) mRNA expression of TLR4, p38 and NF-κB in colonic tissues. (D) Secreted TNF-α, TGF-β and IL-10 levels in colonic tissues. *P<0.05 vs. *E. coli*-infected Ednrb$^{-/-}$ group; #P<0.05 vs. WT and *E. coli*-infected WT groups; &P<0.05 vs. *E. coli*-infected WT and Ednrb$^{-/-}$ groups. Ednrb, endothelin receptor B; WT, wild-type; p-, phosphorylated; TLR, Toll-like receptor.

in the intestinal mucosal barrier in both WT+siRNA-NC and si-TLR4-transfected WT mice 5 weeks after *E. coli* infection (Fig. 5A and B). By contrast, Ednrb$^{-/-}$ mice exhibited a substantially decreased density of F-actin protein and severely disordered tight junction structures in response to *E. coli* infection (Fig. 5C). Of note, TLR4 knockdown in Ednrb$^{-/-}$ mice gradually increased the density of F-actin and partly reversed tight junction integrity (Fig. 5D).

TLR4 knockdown reduces inflammatory response in Ednrb$^{-/-}$ mice and suppresses downstream TLR4/p-p38/NF-κB signaling. To ascertain whether TLR4/p-p38/NF-κB signaling was critical to the progression of HAEC, TLR4-mediated downstream pathways and inflammatory cytokines were examined following TLR4 knockdown in WT and Ednrb$^{-/-}$ mice after *E. coli* infection. The activation of downstream TLR4/p-p38/NF-κB signaling pathways, including NF-κB

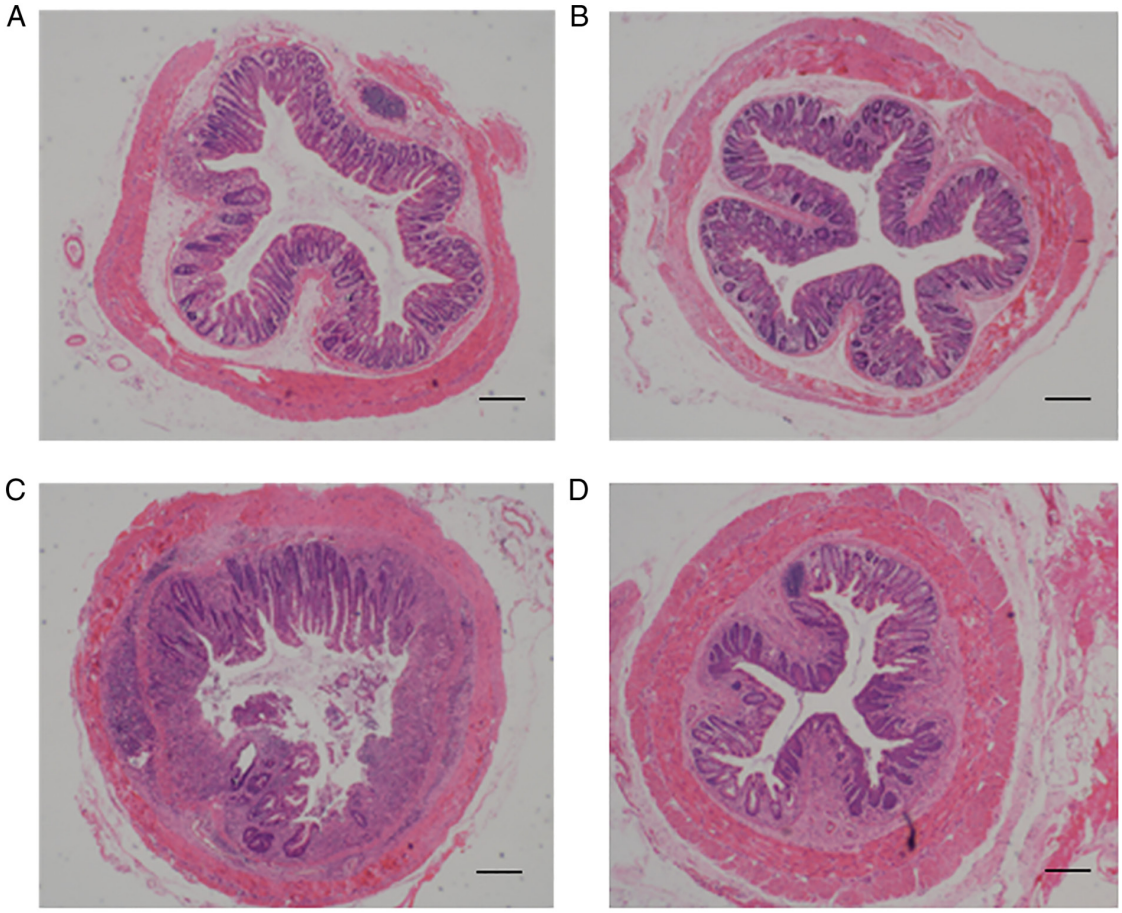

Figure 4. TLR4 knockdown reverses intestinal inflammation. The colon tissues were collected at 5 weeks after modeling. (A) WT+siRNA-NC+*E. coli* group; (B) si-TLR4-transfected WT+*E. coli* group; (C) Ednrb$^{-/-}$+*E. coli* group; and (D) si-TLR4-transfected Ednrb$^{-/-}$+*E. coli* group. Hematoxylin and eosin staining was performed to assess histopathological changes (n=5 per group; scale bar, 100 μm). Ednrb, endothelin receptor B; WT, wild-type; siRNA, small interfering RNA; NC, negative control; si-TLR4, siRNA targeting TLR4; TLR, Toll-like receptor.

and p-p38/p38, was further examined. As presented in Fig. 6A, transfection of both WT and Ednrb$^{-/-}$ mice with si-TLR4 efficiently knocked down TLR4 protein expression. The TLR4 protein was significantly upregulated in *E. coli*-infected Ednrb$^{-/-}$ mice, which were subjected to a rescue experiment (P<0.05 vs. WT+siRNA-NC and *E. coli*-infected Ednrb$^{-/-}$+si-TLR4 mice). Of note, TLR4 knockdown in *E. coli*-infected Ednrb$^{-/-}$ mice markedly suppressed NF-κB and p-p38 expression at the protein level (P<0.05 vs. *E. coli*-infected Ednrb$^{-/-}$ mice; Fig. 6B and C). Furthermore, TLR4 knockdown significantly attenuated TNF-α, TGF-β and IL-10 expression in *E. coli*-infected Ednrb$^{-/-}$ mice (P<0.05 vs. *E. coli*-infected Ednrb$^{-/-}$ mice; Fig. 6D). However, the expression levels of p-p38, TNF-α, TGF-β and IL-10 were increased in si-TLR4-transfected *E. coli*-infected Ednrb$^{-/-}$ mice, compared with those in si-TLR4-transfected *E. coli*-infected WT mice (P<0.05; Fig. 6C and D).

Ednrb suppresses MM proliferation via activation of TLR4/p-p38/NF-κB signaling to promote inflammation. As presented in Fig. 7A-D, a large number of pseudopods were observed in both WT and si-TLR4-transfected Ednrb$^{-/-}$ MMs in response to *E. coli* infection compared with the WT+siRNA-NC group. By contrast, a small number of pseudopods was present in Ednrb$^{-/-}$ MMs upon *E. coli* infection. The proliferative ability of MMs in the Ednrb$^{-/-}$ group was significantly decreased compared with that in the Ednrb$^{-/-}$+si-TLR4 group (P<0.05; Fig. 7E). WT MMs exhibited upregulated expression of NF-κB and p-p38 with significantly increased TGF-β and TNF-α levels, but diminished IL-10 levels in response to *E. coli* infection compared with WT+siRNA-NC MMs (P<0.05; Fig. 8A-C). Of note, in the presence of *E. coli* infection, Ednrb$^{-/-}$ MMs exhibited downregulated expression of NF-κB and p-p38, as well as lower TNF-α and TGF-β levels and increased IL-10 levels (P<0.05 vs. WT and Ednrb$^{-/-}$+si-TLR4; Fig. 8B and C). Knockdown of TLR4 in Ednrb$^{-/-}$ MMs resulted in substantially increased levels of TNF-α and TGF-β, and decreased levels of IL-10 upon *E. coli* infection (P<0.05 vs. Ednrb$^{-/-}$; Fig. 8B and C).

Discussion

HAEC may occur at any time prior to, during or even after endorectal pull-through surgery, which is the definitive procedure for HSCR (25). There exists a wide variation in the reported incidence of HAEC, which occurs in 2-33% of patients with common-type and 50% of patients with long-type HSCR (4). Clinically, HAEC is characterized by discomfort, a loss of appetite, abdominal distention, loose foul-smelling stools, fever and sepsis (26). Previous studies suggested that postoperative

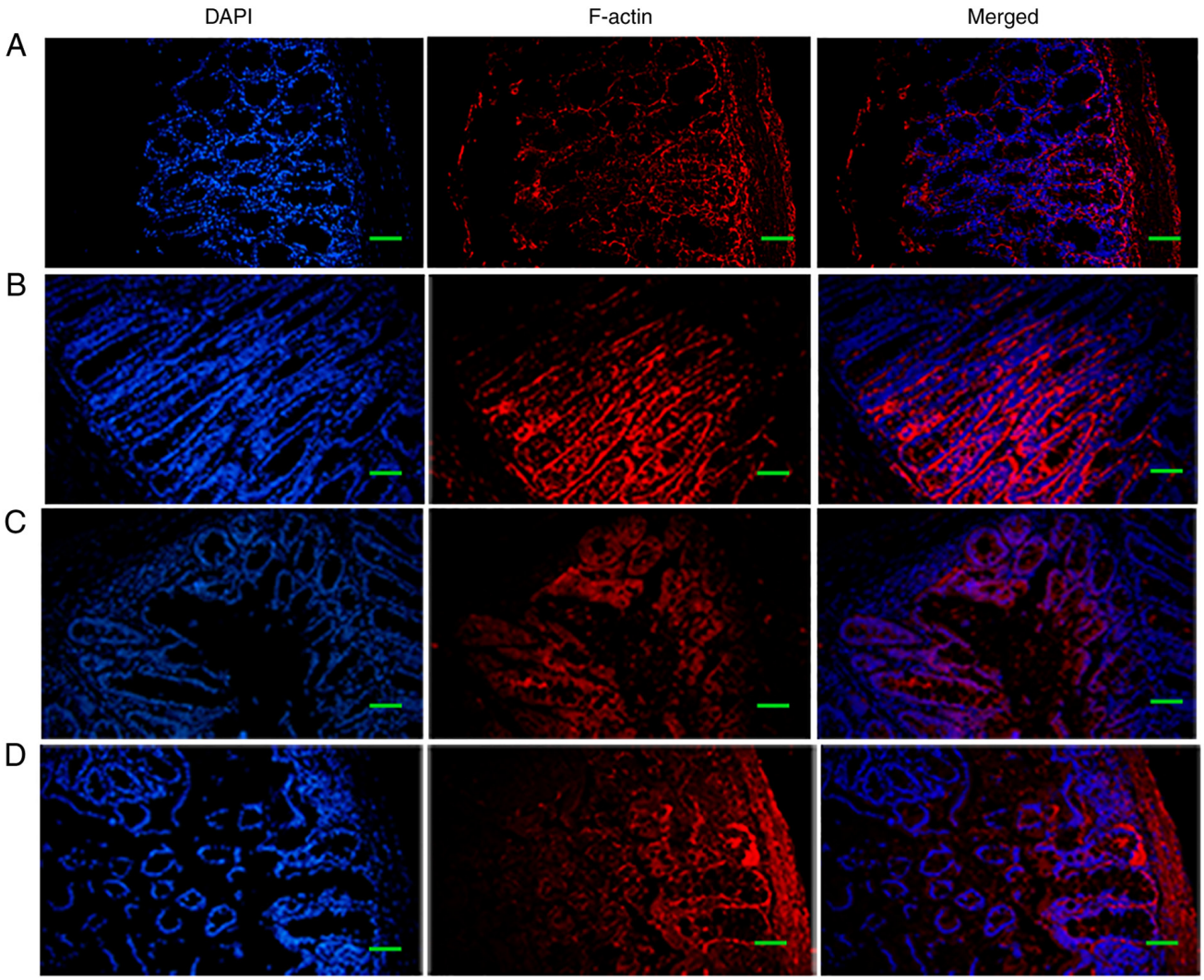

Figure 5. Representative F-actin immunofluorescence staining images of colonic sections. (A) WT+siRNA-NC+*E. coli* group; (B) si-TLR4-transfected WT+*E. coli* group; (C) Ednrb$^{-/-}$+*E. coli* group; and (D) si-TLR4-transfected Ednrb$^{-/-}$+*E. coli* group (n=5 per group; scale bar, 200 μm). Ednrb, endothelin receptor B; WT, wild-type; siRNA, small interfering RNA; NC, negative control; si-TLR4, siRNA targeting TLR4; TLR, Toll-like receptor.

HAEC was related to surgical factors, such as anastomotic stricture or leak, and bowel obstructions (1,5,11,27-29). More recent studies have indicated that the pathogenesis of HAEC is related to the mucosal barrier, intestinal microbiota and immune function (10,30,31). At least partly due to the wide use of Ednrb$^{-/-}$ animal models in HAEC research, the order in which these HAEC-related etiological features change is gradually becoming increasingly understood, which has promoted improvements in the treatment and prevention of HAEC (32-34). A previous multicenter study determined that HAEC patients exhibited a reduced abundance of the phyla *Firmicutes* and an increased abundance of the phyla *Bacteroidetes* and *Proteobacteria*, by comparing the bacterial microbiome composition of pediatric patients with HSCR to those who had a history of HAEC (9). These results strongly indicate a dysequilibrium in the gut microbial ecosystem of patients with HAEC, such that the dominance of bacteria (*E. coli*) predisposes a patient to the development of HAEC.

In the present study, *E. coli* JM83 was used as the pathogenic bacterium to infect the intestines of Ednrb$^{-/-}$ mice to establish a mouse model of HAEC. A previous study reported that Ednrb$^{-/-}$ mice developed HAEC on post-natal days 24-26 and 100% mortality was recorded by day 28 after birth (32). Clinical histopathological features of patients with HAEC mainly include colon crypt dilatation, mucin retention, enterocyte adherence of bacteria, epithelial damage, leukocyte infiltration and ulceration, and in the terminal stages, transmural necrosis and perforation (35,36). In the present study, the histopathological results indicated that a certain amount of inflammatory cells infiltrated the mucosa and submucosa of the intestinal wall, and even abscesses were observed in *E. coli* JM83-infected Ednrb$^{-/-}$ mice, in accordance with the manifestation observed in humans. Ten Ednrb$^{-/-}$ mice developed HAEC 3 weeks after *E. coli* JM83 infection; eight mice survive for more than 5 weeks, with two mice dying of abdominal distention, diarrhea and dehydration; the 80% survival rate was higher than that reported in a previous study (20).

A previous study indicated passive transport of *E. coli* through the mucosal barrier in Ednrb$^{-/-}$ mice and *E. coli* transport was significantly reduced in the proximal colon compared with the distal colon (37). Previous studies also suggested that the dysfunction of the intestinal epithelium contributed

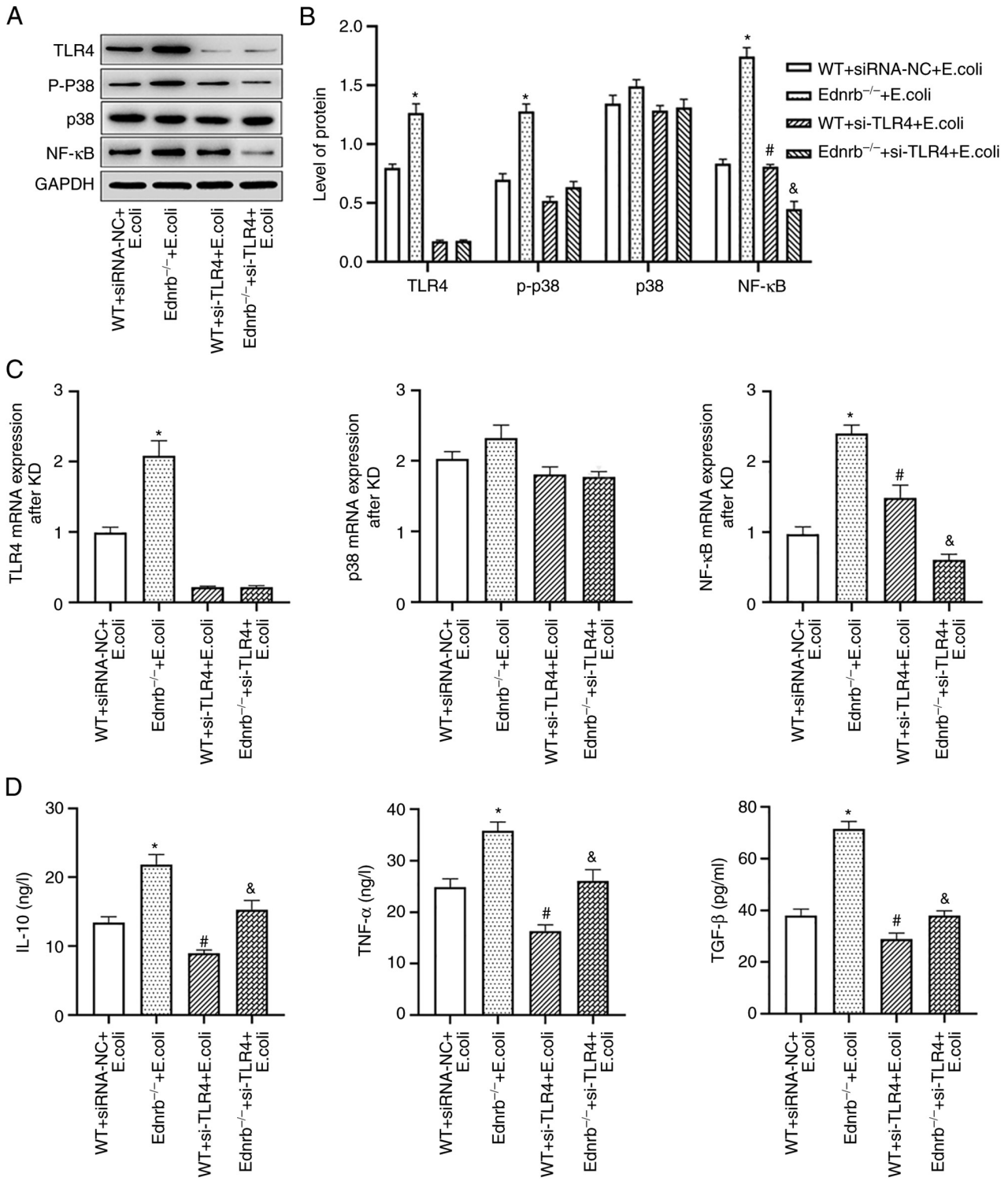

Figure 6. TLR4 knockdown inhibits the secretion of intestinal inflammatory cytokines. (A and B) Western blot analysis of TLR4, p-p38, p38 and NF-κB protein expression levels in colonic tissues. (A) Representative western blot image and (B) quantified expression levels. (C) mRNA expression levels of TLR4, p38 and NF-κB in colonic tissues. (D) Secreted TNF-α, TGF-β and IL-10 expression in the colonic tissues. *P<0.05 vs. WT+siRNA-NC+*E. coli*, Ednrb$^{-/-}$+*E. coli* and si-TLR4-transfected Ednrb$^{-/-}$+*E. coli* groups; #P<0.05 vs. si-TLR4-transfected Ednrb$^{-/-}$+*E. coli* group; &P<0.05 vs. WT+siRNA-NC+*E. coli*, si-TLR4-transfected WT+*E. coli* and Ednrb$^{-/-}$+*E. coli* groups (n=5 per group). Ednrb, endothelin receptor B; WT, wild-type; p-, phosphorylated; siRNA, small interfering RNA; NC, negative control; si-TLR4, siRNA targeting TLR4; TLR, Toll-like receptor.

to the reduction in expression and changes in distribution of F-actin, influencing barrier function and increasing permeability (24,38). The results of the present study indicated that the expression of F-actin gradually decreased with the activation of the TLR4/p-p38/NF-κB signaling pathway and thus eventually led to intestinal mucosal damage, and the levels of IL-10 gradually increased, consistent with the degree of intestinal barrier damage. These results are supported by those of previous studies (39,40), suggesting that IL-10 is a pleiotropic cytokine, the activity of which attempts to limit

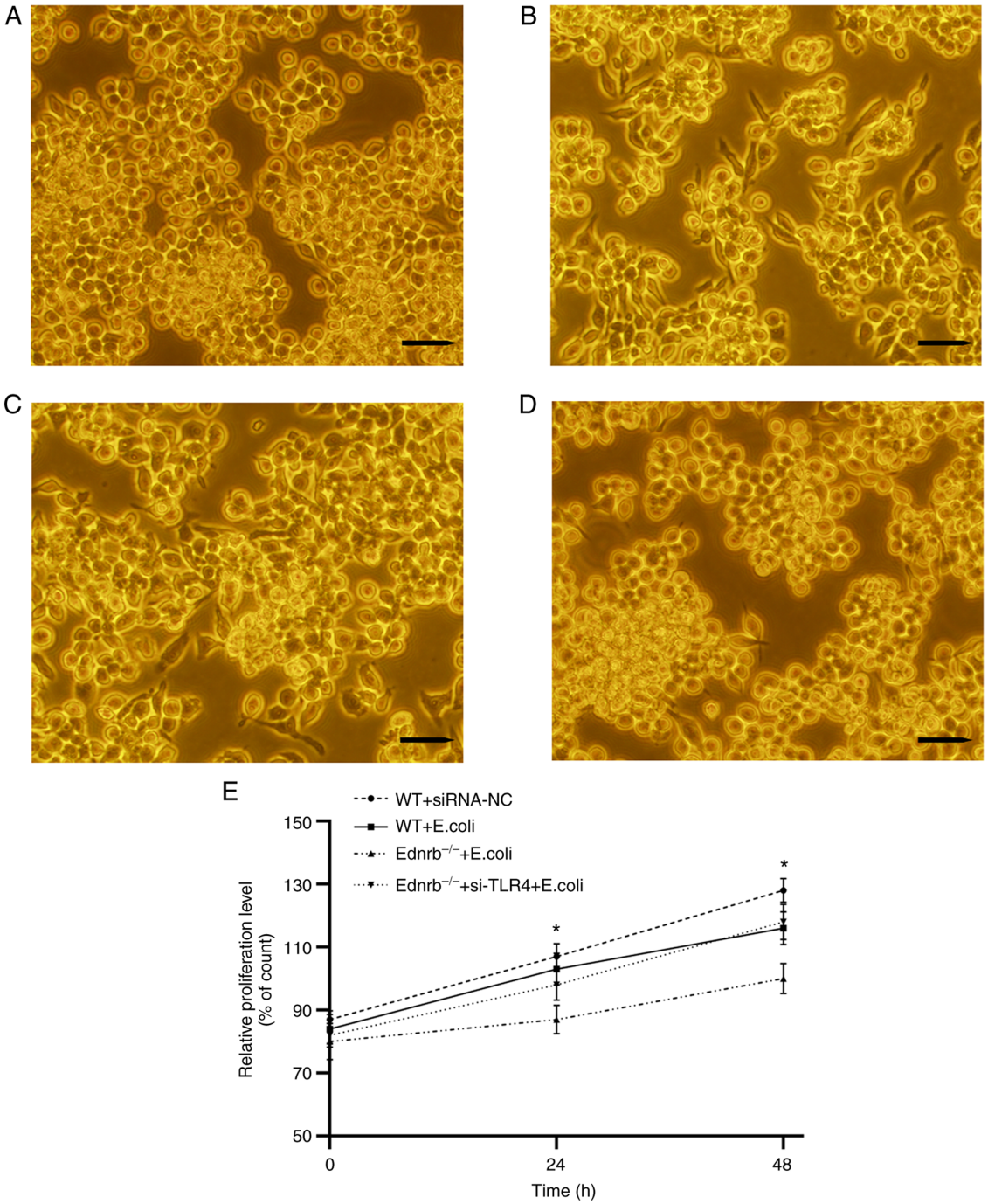

Figure 7. Proliferation of MM cells was assessed using a CCK-8 assay. Images of MM cells from the (A) WT+siRNA-NC group; (B) WT+*E. coli* group; (C) Ednrb$^{-/-}$+*E. coli* group; and (D) si-TLR4-transfected Ednrb$^{-/-}$+*E. coli* group (scale bar, 50 μm). (E) CCK-8 assay. *P<0.05 Ednrb$^{-/-}$+*E. coli* vs. si-TLR4-transfected Ednrb$^{-/-}$+*E. coli* groups. Ednrb, endothelin receptor B; WT, wild-type; siRNA, small interfering RNA; NC, negative control; si-TLR4, siRNA targeting TLR4; TLR, Toll-like receptor; MM, Muscularis macrophage; CCK-8, Cell Counting Kit-8.

inflammatory responses. TNF-α and TGF-β expression were also significantly increased in HAEC mice in the present study, which supported the finding of a previous study that the secretion of pro-inflammatory cytokines, such as TNF-α, IFN-γ, TGF-β and IL-6, and other inflammatory mediators and the resultant cascade reactions aggravate inflammation and destroy intestinal barrier function in patients with HAEC (41). Certain studies have indicated that IL-10 decreased the secretion of TNF-α. However, the high levels of TNF-α reported in inflammatory bowel diseases are produced by recruitment of immune cells rather than by resident colitogenic cells (41,42). Studies have reported that TLR4 activated by bacteria may be a major mediator of activating intestinal mucosal immunity, progression of intestinal inflammation and promotion of the immune response (16,43). Therefore, the results of the present study correspond with the fact that HAEC may occur after postoperative pull-through surgery.

The TLR4/p-p38/NF-κB signaling pathway is transmitted through adaptor proteins and signaling through MyD88 may be necessary to drive phagocytosis (15,44,45). Studies

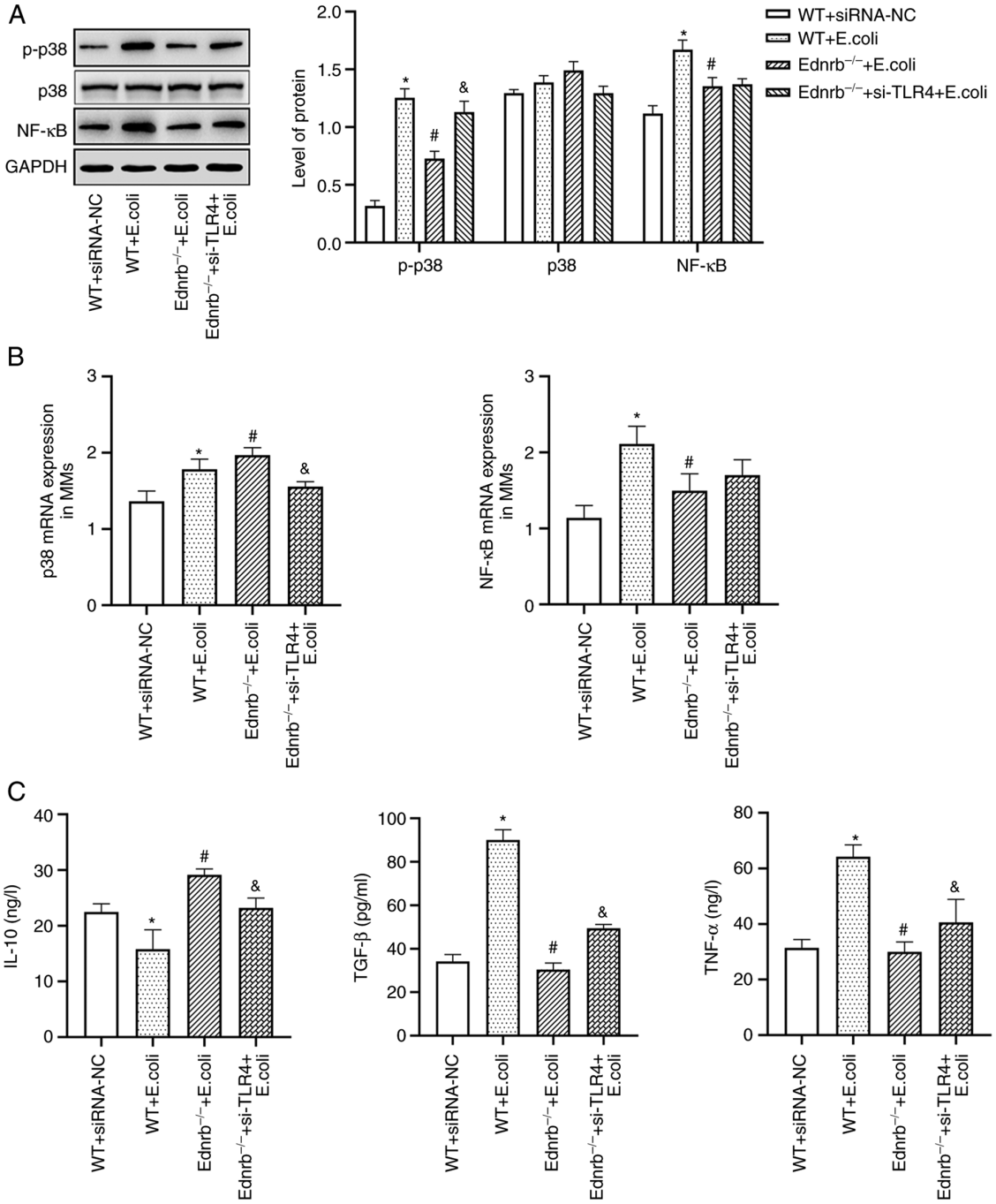

Figure 8. TLR4/p-p38/NF-κB signaling is primarily responsible for induction of the anti-inflammatory activity in MMs. (A) Protein expression levels of NF-κB, p38 and p-p38. (B) mRNA levels of p38 and NF-κB. (C) Secretion levels of TNF-α, TGF-β and IL-10 in the culture supernatants. *P<0.05 vs. WT+siRNA-NC+*E. coli*, Ednrb$^{-/-}$+*E. coli* and si-TLR4-transfected Ednrb$^{-/-}$+*E. coli* groups; #P<0.05 vs. si-TLR4-transfected Ednrb$^{-/-}$+*E. coli* group; &P<0.05 vs. WT+siRNA-NC, WT+*E. coli* and Ednrb$^{-/-}$+*E. coli* groups (n=5 per group). Ednrb, endothelin receptor B; TLR, Toll-like receptor; NC, negative control; si-TLR4, siRNA targeting TLR4; WT, wild-type; p-, phosphorylated; siRNA, small interfering RNA; MM, Muscularis macrophage.

have indicated that the primary function of TLR4 signaling in macrophages is to induce inflammatory responses and protect the host from pathogenic bacteria (19,46). The *in vivo* experiments of the present study revealed that TLR4 protein expression was upregulated in the colon for 3 weeks following stimulation with *E. coli* JM83. TLR4 stimulated NF-κB through MyD88 in a mouse model and the levels of NF-κB and p-p38/p38 were increased in the colon wall following stimulation with *E. coli* JM83. Likewise, NF-κB induced an increase in TNF-α and TGF-β expression with the degree of enterocolitis in Ednrb$^{-/-}$ mice, and therefore eventually led to intestinal mucosal damage. The above results indicate that the TLR4/p-p38/NF-κB signaling pathway has a central role in the initiation of innate cellular immune responses and in the development of subsequent adaptive immune responses to invading bacterial infection, and eventually promote intestinal mucosal tissue damage in HAEC. This process is consistent with the pathogenesis of inflammatory bowel disease in previous adult studies (47,48). By contrast, mucosal barrier integrity was maintained without the development of enterocolitis following

TLR4 knockdown. A previous study indicated that upregulated TLR4 expression is related to mortality in a model of sepsis (46).

However, siRNA-mediated knockdown of TLR4 to inhibit TLR4/p-p38/NF-κB signaling reversed the inflammatory effects caused by *E. coli* infection, indicating that TLR4/p-p38/NF-κB signaling has a central role in maintaining the balance of gut homeostasis during the pathogenesis of HAEC. Under certain conditions, this downregulation of TLR4 signaling may ameliorate the degree of immune-mediated enterocolitis, providing a novel idea for the treatment and prevention of HAEC.

The limitation of the present study was that it did not analyze the side effects of inhibition of the TLR4/p-p38/NF-κB signaling pathway. Since the TLR4 receptor is expressed in a number of cells, we aim to focus on intestine-specific inhibitors of the TLR4/p-p38/NF-κB pathway and assess their protective effect on HAEC in future studies.

In conclusion, the present study highlighted the response of the intestinal mucosal barrier to HAEC induced by pathogenic *E. coli*. In addition, the activation of TLR4/p-p38/NF-κB signaling in Ednrb$^{-/-}$ mice by *E. coli* JM83 led to the development of inflammation and the underlying mechanism was indicated to be this signaling pathway. Furthermore, inhibition of TLR4/p-p38/NF-κB signaling may be of potential benefit for the treatment and prevention of HAEC, highlighting a novel means for improving intestinal mucosal integrity.

Acknowledgements

Not applicable.

Funding

This work was supported by the Joint Fund of the Department of Guizhou Science and Technology of China (Guizhou, China; grant nos. 20177100, 20204Y005 and ZK2021361).

Availability of data and materials

The datasets used and/or analyzed during the present study are available from the corresponding author on reasonable request.

Authors' contributions

ZZ performed the majority of experiments, analyzed the data and wrote, reviewed and edited the manuscript. MG, CT, LH and YG curated and analyzed the data. JW and YL conceived and designed the experiments and contributed to the analytical tools. All of the authors have read and approved the final manuscript. JW and YL confirm the authenticity of all the raw data.

Ethics approval and consent to participate

All animal experimental protocols complied with the Guide for the Care and Use of Laboratory Animals published by the National Institutes of Health. The present study was approved by the Institutional Animal Research Committee of Zunyi Medical University (Guizhou, China; approval no. IACUC-20191025028).

Patient consent for publication

Not applicable.

Competing interests

The authors declare that they have no competing interests.

References

1. Le-Nguyen A, Righini-Grunder F, Piché N, Faure C and Aspirot A: Factors influencing the incidence of Hirschsprung associated enterocolitis (HAEC). J Pediatr Surg 54: 959-963, 2019.
2. Nakamura H, Lim T and Puri P: Probiotics for the prevention of Hirschsprung-associated enterocolitis: A systematic review and meta-analysis. Pediatr Surg Int 34: 189-193, 2018.
3. Fang YF, Bai JX, Zhang B, Wu DM, Lin Y and Liu MK: Laparoscopic Soave procedure for long-segment Hirschsprung's disease-single-center experience. Videosurgery Miniinv 15: 234-238, 2020.
4. Austin KM: The pathogenesis of Hirschsprung's disease-associated enterocolitis. Semin Pediatr Surg 21: 319-327, 2012.
5. Cheng S, Wang J, Pan W, Yan W, Shi J, Guan W, Wang Y and Cai W: Pathologically assessed grade of Hirschsprung-associated enterocolitis in resected colon in children with Hirschsprung's disease predicts postoperative bowel function. J Pediatr Surg 52: 1776-1781, 2017.
6. Frykman PK, Nordenskjöld A, Kawaguchi A, Hui TT, Granström AL, Cheng Z, Tang J, Underhill DM, Iliev I, Funari VA, *et al*: Characterization of bacterial and fungal microbiome in children with Hirschsprung disease with and without a history of enterocolitis: A multicenter study. PLoS One 10: e0124172, 2015.
7. Li Y, Poroyko V, Yan Z, Pan L, Feng Y, Zhao P, Xie Z and Hong L: Characterization of intestinal microbiomes of Hirschsprung's disease patients with or without enterocolitis using illumina-MiSeq high-throughput sequencing. PLoS One 11: e0162079, 2016.
8. Neuvonen MI, Korpela K, Kyrklund K, Salonen A, de Vos W, Rintala RJ and Pakarinen MP: Intestinal microbiota in Hirschsprung disease. J Pediatr Gastroenterol Nutr 67: 594-600, 2018.
9. Prato AP, Bartow-McKenney C, Hudspeth K, Mosconi M, Rossi V, Avanzini S, Faticato MG, Ceccherini I, Lantieri F, Mattioli G, *et al*: A metagenomics study on Hirschsprung's disease associated enterocolitis: Biodiversity and gut microbial homeostasis depend on resection length and patient's clinical history. Front Pediatr 7: 326, 2019.
10. Singer G, Kashofer K, Castellani C and Till H: Hirschsprung's associated enterocolitis (HAEC) personalized treatment with probiotics based on gene sequencing analysis of the fecal microbiome. Case Rep Pediatr 2018: 3292309, 2018.
11. Tang W, Su Y, Yuan C, Zhang Y, Zhou L, Peng L, Wang P, Chen G, Li Y, Li H, *et al*: Prospective study reveals a microbiome signature that predicts the occurrence of post-operative enterocolitis in Hirschsprung disease (HSCR) patients. Gut Microbes 11: 842-854, 2020.
12. Bigorgne AE, John B, Ebrahimkhani MR, Shimizu-Albergine M, Campbell JS and Crispe IN: TLR4-dependent secretion by hepatic stellate cells of the neutrophil-chemoattractant CXCL1 mediates liver response to gut microbiota. PLoS One 11: e0151063, 2016.
13. Cheng Y, Zhu Y, Huang X, Zhang W, Han Z and Liu S: Association between TLR2 and TLR4 gene polymorphisms and the susceptibility to inflammatory bowel disease: A meta-analysis. PLoS One 10: e0126803, 2015.
14. Płóciennikowska A, Hromada-Judycka A, Borzęcka K and Kwiatkowska K: Co-operation of TLR4 and raft proteins in LPS-induced pro-inflammatory signaling. Cell Mol Life Sci 72: 557-581, 2015.
15. Rosadini CV, Zanoni I, Odendall C, Green ER, Paczosa MK, Philip NH, Brodsky IE, Mecsas J and Kagan JC: A single bacterial immune evasion strategy dismantles both MyD88 and TRIF signaling pathways downstream of TLR4. Cell Host Microbe 18: 682-693, 2015.

16. Leaphart CL, Cavallo J, Gribar SC, Cetin S, Li J, Branca MF, Dubowski TD, Sodhi CP and Hackam DJ: A critical role for TLR4 in the pathogenesis of necrotizing enterocolitis by modulating intestinal injury and repair. J Immunol 179: 4808-4820, 2007.
17. Liu S, Gallo DJ, Green AM, Williams DL, Gong X, Shapiro RA, Gambotto AA, Humphris EL, Vodovotz Y and Billiar TR: Role of toll-like receptors in changes in gene expression and NF-kappa B activation in mouse hepatocytes stimulated with lipopolysaccharide. Infect Immun 70: 3433-3442, 2002.
18. Gibson DL, Ma C, Rosenberger CM, Bergstrom KS, Valdez Y, Huang JT, Khan MA and Vallance BA: Toll-like receptor 2 plays a critical role in maintaining mucosal integrity during citrobacter rodentium-induced colitis. Cell Microbiol 10: 388-403, 2008.
19. Zhang J, Zheng Y, Luo Y, Du Y, Zhang X and Fu J: Curcumin inhibits LPS-induced neuroinflammation by promoting microglial M2 polarization via TREM2/TLR4/NF-κB pathways in BV2 cells. Mol Immunol 116: 29-37, 2019.
20. Porokuokka LL, Virtanen HT, Lindén J, Sidorova Y, Danilova T, Lindahl M, Saarma M and Andressoo JO: Gfra1 underexpression causes Hirschsprung's disease and associated enterocolitis in mice. Cell Mol Gastroenterol Hepatol 7: 655-678, 2019.
21. Frykman PK, Cheng Z, Wang X and Dhall D: Enterocolitis causes profound lymphoid depletion in endothelin receptor B- and endothelin 3-null mouse models of Hirschsprung-associated enterocolitis. Eur J Immunol 45: 807-817, 2015.
22. Livak KJ and Schmittgen TJ: Analysis of relative gene expression data using real-time quantitative PCR and the 2(-Delta Delta C(T)) method. Methods 25: 402-408, 2001.
23. Muller PA, Koscsó B, Rajani GM, Stevanovic K, Berres ML, Hashimoto D, Mortha A, Leboeuf M, Li XM, Mucida D, *et al*: Crosstalk between muscularis macrophages and enteric neurons regulates gastrointestinal motility. Cell 158: 300-313, 2014.
24. Ye X and Sun M: AGR2 ameliorates tumor necrosis factor-α-induced epithelial barrier dysfunction via suppression of NF-κB p65-mediated MLCK/p-MLC pathway activation. Int J Mol Med 39: 1206-1214, 2017.
25. Mao YZ, Tang ST and Li S: Duhamel operation vs transanal endorectal pull-through procedure for Hirschsprung disease: A systematic review and meta-analysis. J Pediatr Surg 53: 1710-1715, 2018.
26. Dore M, Vilanova Sanchez A, Triana Junco P, Barrena S, De Ceano-Vivas M, Jimenez Gomez J, Andres Moreno AM, Lopez Santamaria M and Martinez L: Reliability of the Hirschsprung-associated enterocolitis score in clinical practice. Eur J Pediatr Surg 29: 132-137, 2019.
27. Zhang X, Li L, Li SL, Li SX, Wang XY and Tang ST: Primary laparoscopic endorectal pull-through procedure with or without a postoperative rectal tube for Hirschsprung disease: A multicenter perspective study. J Pediatr Surg 55: 381-386, 2020.
28. Pruitt LCC, Skarda DE, Rollins MD and Bucher BT: Hirschsprung-associated enterocolitis in children treated at US children's hospitals. J Pediatr Surg 55: 535-540, 2020.
29. Taylor MA, Bucher BT, Reeder RW, Avansino JR, Durham M, Calkins CM, Wood RJ, Levitt MA, Drake K and Rollins MD: Comparison of Hirschsprung disease characteristics between those with a history of postoperative enterocolitis and those without: Results from the pediatric colorectal and pelvic learning consortium. Eur J Pediatr Surg 31: 207-213, 2021.
30. Cheng Z, Zhao L, Dhall D, Ruegger PM, Borneman J and Frykman PK: Bacterial microbiome dynamics in post pull-through Hirschsprung-associated enterocolitis (HAEC): An experimental study employing the endothelin receptor B-null mouse model. Front Surg 5: 30, 2018.
31. Halleran DR, Ahmad H, Maloof E, Paradiso M, Lehmkuhl H, Minneci PC, Levitt MA and Wood RJ: Does Hirschsprung-associated enterocolitis differ in children with and without down syndrome? J Surg Res 245: 564-568, 2020.
32. Cheng Z, Wang X, Dhall D, Zhao L, Bresee C, Doherty TM and Frykman PK: Splenic lymphopenia in the endothelin receptor B-null mouse: Implications for Hirschsprung associated enterocolitis. Pediatr Surg Int 27: 145-150, 2011.
33. Fattahi F, Steinbeck JA, Kriks S, Tchieu J, Zimmer B, Kishinevsky S, Zeltner N, Mica Y, El-Nachef W, Zhao H, *et al*: Deriving human ENS lineages for cell therapy and drug discovery in Hirschsprung disease. Nature 531: 105-109, 2016.
34. Soret R, Schneider S, Bernas G, Christophers B, Souchkova O, Charrier B, Righini-Grunder F, Aspirot A, Landry M, Kembel SW, *et al*: Glial cell-derived neurotrophic factor induces enteric neurogenesis and improves colon structure and function in mouse models of Hirschsprung disease. Gastroenterology 159: 1824-1838.e17, 2020.
35. Gosain A, Frykman PK, Cowles RA, Horton J, Levitt M, Rothstein DH, Langer JC and Goldstein AM; American Pediatric Surgical Association Hirschsprung Disease Interest Group: Guidelines for the diagnosis and management of Hirschsprung-associated enterocolitis. Pediatr Surg Int 33: 517-521, 2017.
36. Mattar AF, Coran AG and Teitelbaum DH: MUC-2 mucin production in Hirschsprung's disease: Possible association with enterocolitis development. J Pediatr Surg 38: 417-421, 2003.
37. Yildiz HM, Carlson TL, Goldstein AM and Carrier RL: Mucus Barriers to microparticles and microbes are altered in Hirschsprung's disease. Macromol Biosci 15: 712-718, 2015.
38. Song H, Zhang J, He W, Wang P and Wang F: Activation of cofilin increases intestinal permeability via depolymerization of F-actin during hypoxia in vitro. Front Physiol 10: 1455, 2019.
39. Liu D, Yin X, Olyha SJ, Nascimento MSL, Chen P, White T, Gowthaman U, Zhang T, Gertie JA, Zhang B, *et al*: IL-10-dependent crosstalk between murine marginal zone B cells, macrophages, and CD8α$^+$ dendritic cells promotes listeria monocytogenes infection. Immunity 51: 64-76.e7, 2019.
40. Zigmond E, Bernshtein B, Friedlander G, Walker CR, Yona S, Kim KW, Brenner O, Krauthgamer R, Varol C, Müller W and Jung S: Macrophage-restricted interleukin-10 receptor deficiency, but not IL-10 deficiency, causes severe spontaneous colitis. Immunity 40: 720-733, 2014.
41. Schreurs RRCE, Baumdick ME, Sagebiel AF, Kaufmann M, Mokry M, Klarenbeek PL, Schaltenberg N, Steinert FL, van Rijn JM, Drewniak A, *et al*: Human fetal TNF-α-cytokine-producing CD4$^+$ effector memory T cells promote intestinal development and mediate inflammation early in life. Immunity 50: 462-476.e8, 2019.
42. Ahn J, Son S, Oliveira SC and Barber GN: STING-dependent signaling underlies IL-10 controlled inflammatory colitis. Cell Rep 21: 3873-3884, 2017.
43. Tan Y, Zanoni I, Cullen TW, Goodman AL and Kagan JC: Mechanisms of toll-like receptor 4 endocytosis reveal a common immune-evasion strategy used by pathogenic and commensal bacteria. Immunity 43: 909-922, 2015.
44. Wang W, Weng J, Yu L, Huang Q, Jiang Y and Guo X: Role of TLR4-p38 MAPK-Hsp27 signal pathway in LPS-induced pulmonary epithelial hyperpermeability. BMC Pulm Med 18: 178, 2018.
45. Yang D, Li S, Duan X, Ren J, Liang S, Yakoumatos L, Kang Y, Uriarte SM, Shang J, Li W and Wang H: TLR4 induced Wnt3a-Dvl3 restrains the intensity of inflammation and protects against endotoxin-driven organ failure through GSK3β/β-catenin signaling. Mol Immunol 118: 153-164, 2020.
46. Zhang Y, Lu Y, Ma L, Cao X, Xiao J, Chen J, Jiao S, Gao Y, Liu C, Duan Z, *et al*: Activation of vascular endothelial growth factor receptor-3 in macrophages restrains TLR4-NF-κB signaling and protects against endotoxin shock. Immunity 40: 501-514, 2014.
47. Meroni E, Stakenborg N, Viola MF and Boeckxstaens GE: Intestinal macrophages and their interaction with the enteric nervous system in health and inflammatory bowel disease. Acta Physiol (Oxf) 225: e13163, 2019.
48. Shouval DS, Biswas A, Goettel JA, McCann K, Conaway E, Redhu NS, Mascanfroni ID, Al Adham Z, Lavoie S, Ibourk M, *et al*: Interleukin-10 receptor signaling in innate immune cells regulates mucosal immune tolerance and anti-inflammatory macrophage function. Immunity 40: 706-719, 2014.